



Recent Advances in Discrete Element Modeling of River Ice

Mark Hopkins and Steven F. Daly

ERDC/CRREL

72 Lyme Road

Hanover, NH 03755

Mark.A.Hopkins@erdc.usace.army.mil; Steven.F.Daly@erdc.usace.army.mil

We have used a discrete element model (DEM) closely coupled with an unsteady flow simulation to model the formation of ice jams and to estimate ice forces on structures. In this paper we provide a brief overview of DEM simulation of river ice processes and report on several recent advances. Previous DEM models used uniform sizes for the ice floes. In a recent study we estimated the magnitude and direction of ice forces on piers of a proposed bridge, and investigated the likelihood of a range of possible pier designs to cause ice jam formation. Three ice conditions were investigated: a single layer of 10-ft-diameter floes; a double layer of 10-ft-diameter floes; and a mixture of 10-, 50-, 100-, and 200-ft-diameter floes. In each case the ice completely covered the surface of the river. The floe dimensions were based on available aerial photographs of the proposed bridge locations. We also developed an efficient "spin-up" procedure to allow efficient initiation of the DEM and the one-dimensional unsteady flow model. On a more fundamental level, we have reviewed the complete equations of motions of ice floes. In general, floes respond to forces imparted by the fluid, forces imparted by other particles, and gravity. We discuss the fluid force equation in detail. It includes the fluid pressure force, the added mass, the drag force, and the buoyancy force. Typically, only the drag and buoyancy forces have been included in previous simulations.

1. Introduction

The simulation of river ice and river ice jams using DEM has been described in a number of previous papers (Daly and Hopkins 2001, 1999, 1996; Hopkins et al 2002, 1999, 1996). In short, we combine a three-dimensional DEM, which explicitly models the dynamics of a system of discrete ice floes with a one-dimensional unsteady flow hydraulic model which includes the influence of the ice on the channel flow. We have found the DEM valuable for addressing questions such as the fundamentals of ice jam formation, forces on ice control structures, the control of ice at locks and dams, the jamming potential of various bridge pier designs, and the ice impacts on bridge piers. The DEM can provide detailed analysis that is not available in other ice jam simulation approaches, and provides results comparable to that provided by physical models.

In this paper we discuss several recent advances. Previous DEM models used uniform sizes for the ice floes. In a recent study we estimated the magnitude and direction of ice forces on piers of a proposed bridge, and investigated the likelihood of a range of possible pier designs to cause ice jam formation. Three ice conditions were investigated: a single layer of 10-ft-diameter floes; a double layer of 10-ft-diameter floes; and a mixture of 10-, 50-, 100-, and 200-ft-diameter floes. In each case the ice completely covered the surface of the river. The floe dimensions were based on available aerial photographs of the proposed bridge locations. The problems associated with the startup of the simulation are also discussed.

On a more fundamental level, we have reviewed the complete equations of motions of ice floes. In general, floes respond to forces imparted by the fluid, forces imparted by other particles, and gravity. We discuss the fluid force equation in detail. It includes the fluid pressure force, the added mass, the drag force, and the buoyancy force. Typically, only the drag and buoyancy forces have been included in previous simulations.

2. Simulating River Ice with Multiple Floe Sizes

2.1 Background A bridge is proposed to cross the Buckland River at Buckland, Alaska. The Buckland River is generally frozen each year from October through May. The interaction of the river ice and the piers of the proposed bridge is an important consideration. During spring breakup of the river ice cover, the moving river ice can exert large forces on the bridge piers, and these forces must be taken into consideration in the design of the piers. The piers may also reduce the ice transport capacity of the river and cause the ice to stop moving or jam. Ice jams can have a dramatic effect on the river flow by blocking the flow area of the channel cross section and reducing the flow capacity of the channel. Ice jams often cause flooding in Buckland. There are 18 recorded ice jam flooding events recorded for Buckland since 1971 (U.S. Army Corps of Engineers, 2001). It is important that the piers of the proposed bridge be designed so that they do not aggravate ice jam flooding in Buckland by restricting ice transport of the Buckland River.

2.2 Ice floe simulation Three ice conditions were investigated: a single layer of 10-ft-diameter floes; a double layer of 10-ft-diameter floes; and a mixture of 10-, 50-, 100-, and 200-ft-diameter floes. To construct the initial configuration of the single layer of 10-ft-diameter floes, ice floes were placed in a large rectangular close-packed hexagonal array with random orientations at a concentration of 62% as shown in Figure 1.

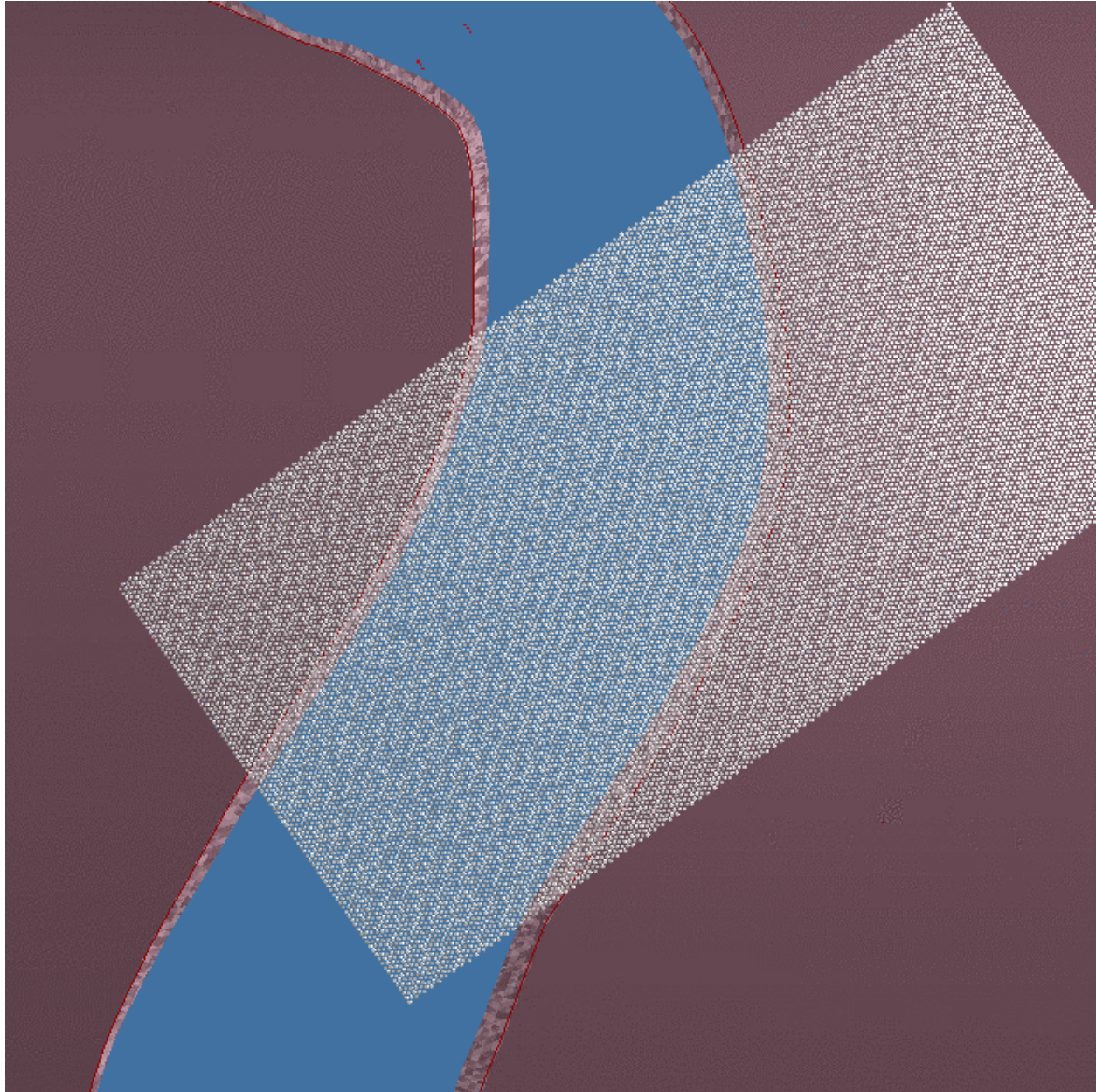


Figure 1. Rectangular Array

The rectangular array was moved to a location in the river upstream of the bridge pier location and rotated to align the array with the channel. The floes lying outside the channel were removed. The remaining 7224 floes were placed at the water surface and allowed to equilibrate

with the initial water surface obtained by spinning up the hydraulic model with no ice present. The process of spinning up the hydraulic model will be discussed in a following section.

The initial configuration of the ice floes in a double layer of 10-ft-diameter floes were obtained by placing an additional layer of 7224 floes over the first layer and dropping them and allowing the ice cover to equilibrate as before.

The initial configuration for a mixture of 10-, 50-, 100-, and 200-ft-diameter floes were obtained by first placing large floes with diameters of 50, 100, and 200 ft randomly in the rectangle such that there was no contact between neighbors to a concentration of 50%. The relative areas occupied by the floes were 26%, 45%, and 29%, respectively (approximated from a drawing furnished by David Shearer based on aerial photographs).

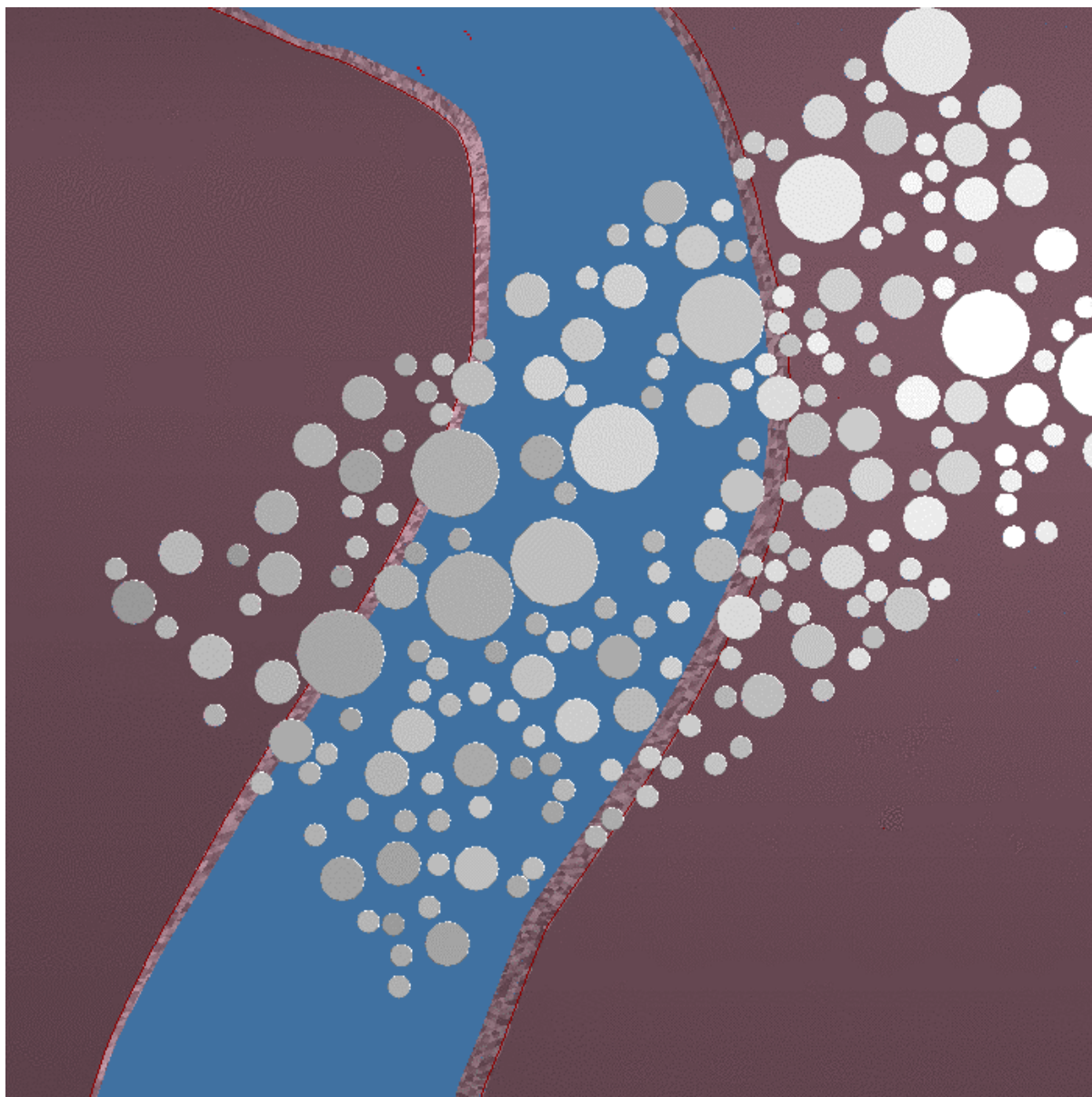


Figure 2. Array of sizes of ice floes in rectangular space.

After placing the large floes in the rectangle, the interstitial areas between the large floes were filled with three layers of small floes. The rectangular area of floes was placed over the river, and the floes that lay outside the channel were removed, leaving 101 large floes and 15,332 small floes as shown in Figure 3

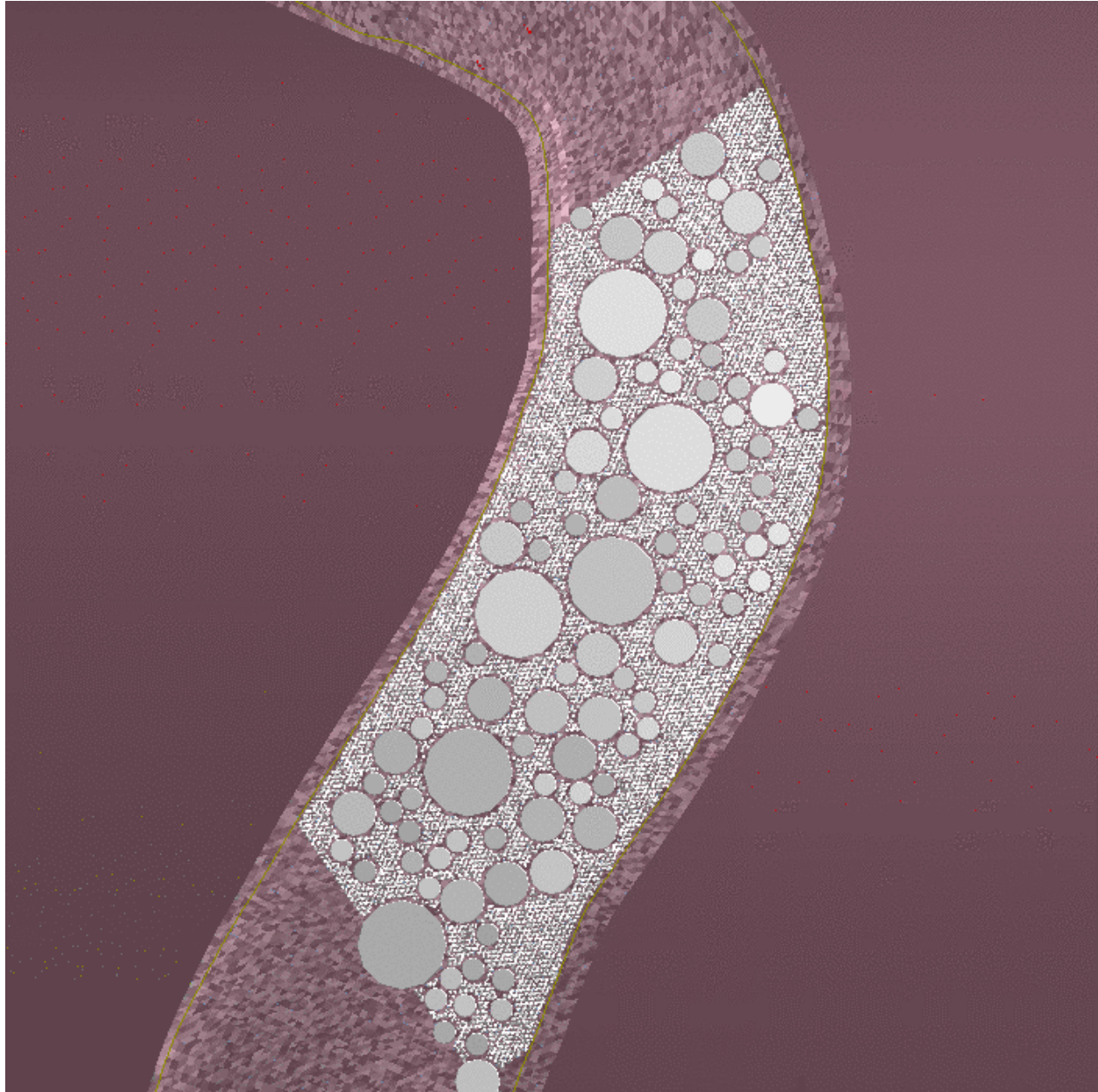


Figure 3. Final ice layout

. The floes were allowed to equilibrate with the initial water surface as before. In each test series the same initial configuration was used to perform a baseline simulation with no bridge piers and a simulation with each of the three proposed bridge pier designs.

2.3 Hydraulic model spin up We discussed the river flow simulation in detail in an earlier paper (Daly and Hopkins, 1998). Briefly the model employs one-dimensional momentum and continuity equations to describe the channel flow. The channel conveyance is used in the momentum equation to estimate the friction losses in the channel. Separate conveyances are found for open-channel flow, for flow under an ice cover, for high-Reynolds-number seepage flow through a porous ice mass, and for fluid transported by the moving ice mass. This allows the simulation to reproduce the types of flow found in ice-covered rivers and ice jams. The momentum and continuity equations are solved simultaneously for the entire river channel using a four-point implicit discretization scheme. Because of the one-dimensional form of the flow equations, all geometric and flow information in the transverse and vertical directions is averaged at each cross section.

Spin-up describes the process of introducing the initial ice floe distribution into the hydraulic model. In all the DEM simulations, the ice is introduced upstream of the region of interest and the ice is transported downstream. However, it is not numerically efficient to gradually introduce the ice into the hydraulic model at the upstream boundary of the model. Rather, we introduce the entire mass of ice into the river channel immediately upstream of the section of interest. Unfortunately, but not unexpectedly, the hydraulic model response to any abrupt change in ice conditions can be dramatic. Early numerical experiments showed that when ice simply appeared in the hydraulic model large persistent transients were created that seriously disrupted the spatial distribution of the ice. We developed the following spin-up procedure to overcome these problems:

1. The ice floes are distributed over a rectangular area as described above in multiple layers, if required. . The rectangular area is moved and rotated to align with the natural channel geometry. Floes that are outside or intersect the channel boundary are discarded.
2. The initial flow conditions are established with a known (or estimated) water surface as the downstream boundary condition and a known discharge as the upstream. The resulting discharge and water surface elevations throughout the hydraulic model converge on steady state values, which reflect the influence of the upstream and downstream boundary conditions.
3. The ice is introduced to the hydraulic model at the mean water surface elevation of the rectangular area. Initially, the discrete ice particle velocities reported to the hydraulic model at each section are equal to the flow velocities at that section. However, the discrete ice particles are prevented from moving in the horizontal plane. The porosity of the ice mass below the water surface is reported to the hydraulic model as 1.0. In this way, the effects of the drag on the underside of the ice, and the blockage effect of the ice are eliminated and no transients are created in the hydraulic model.
4. The ice particles are allowed to move vertically and equilibrate with the water surface elevations established by the hydraulic model throughout the reach with ice.
5. The reported porosity is gradually decreased from 1.0 to the calculated porosity, which generally falls in a range from 0.4 to 0.6. Transients are created in the hydraulic model as a result, but they are generally of minimal amplitude and have short duration. We continue to let the ice particles move vertically and equilibrate with the water surface elevations but restrain the ice particles from moving horizontally.

6. It was found that changes in the hydrostatic pressure acting on each particle as a result of changes in the calculated water surface elevation was not sufficient in itself to move the ice vertically in phase with water surface. It was found necessary to include both changes in hydrostatic pressure about the particles and the vertical water drag. The problem with this is that the one-dimensional hydraulic model can only simulate water velocities that are parallel with the slope of the channel. To overcome this, we estimate a local vertical water velocity based on the rate of change of the water surface elevation at each section. The square of the difference between this vertical velocity and the vertical velocity of each ice particle, with the appropriate sign, is then used to estimate a vertical drag force on the ice particles.
7. The spin-up is continued until the actual porosity of the ice mass below the water is reported to the hydraulic model and the hydraulic model has come to a new steady state. At this time, the ice particles are released and allowed to move horizontally. When the leading edge of the ice mass nears the structure the ice/hydraulic configuration is saved. This configuration is used to begin each simulation that uses those hydraulic conditions.

2.4 Summary of results We investigated the ice forces exerted on the individual bridge piers, the overturning moment exerted on the piers by the ice, and the effect of the bridge piers on the ice passage. were considered. (Hopkins et al 2002) We investigated four pier design alternatives. The alternatives are positioned on two different cross-section lines across the Buckland River located at the sharp bend in the river shown in Figure 4 that is near the village center. The thalweg at the bridge location was approximately 18.6 m.

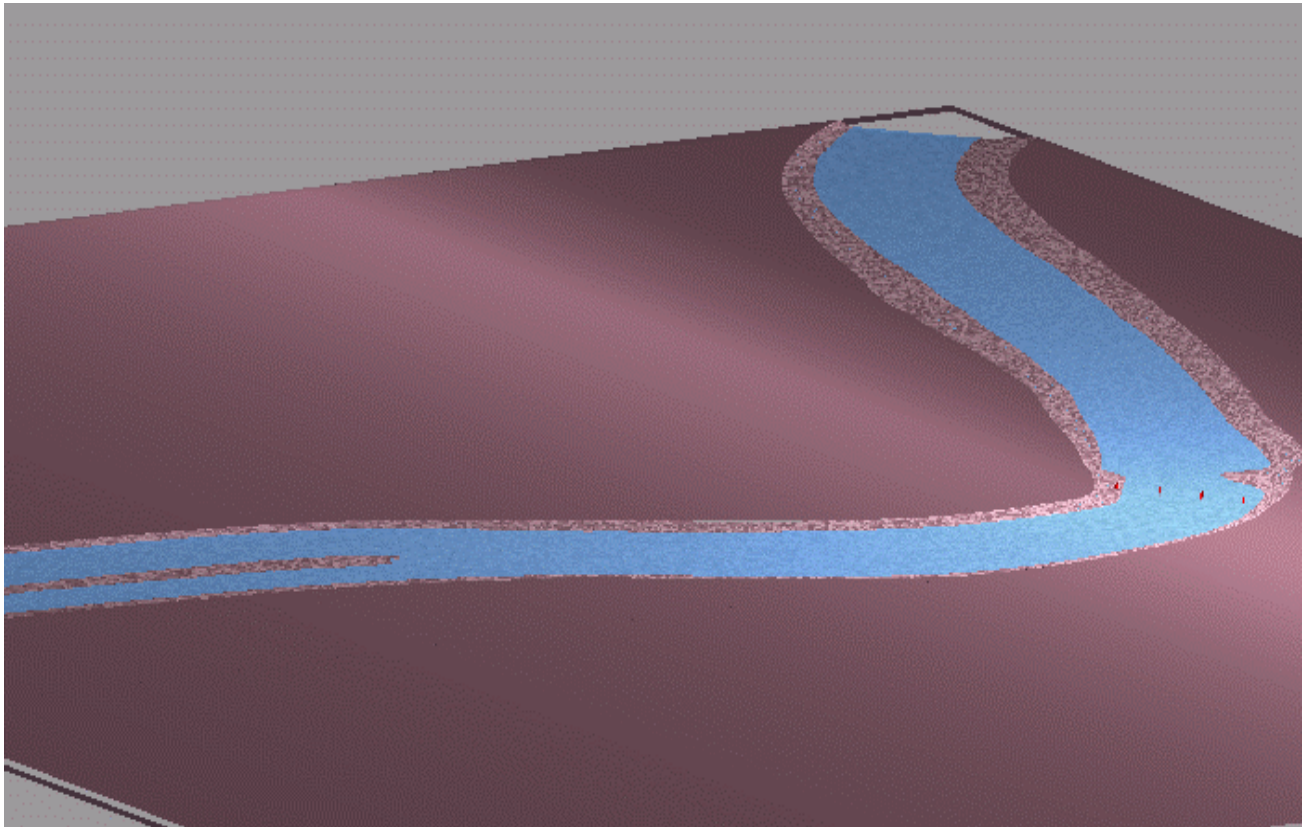


Figure 4. DEM layout showing bridge location.

- Bridge 1: Twelve 1.83-m-diameter piers are clustered in four groups of three piers each on the downstream section line. (See figure 5 for the layout of section lines.) The groups of piers are spaced more or less uniformly across the river.
- Bridge 2: One 2.44-m-diameter pier is located approximately in the middle of the channel on the upstream section line.
- Bridge 3: Two 1.83-m-diameter piers support the bridge on the upstream section line.
- Bridge 4: Two 1.83-m-diameter piers support the bridge on the downstream section line.

Two ice conditions were investigated: a 1-2 m in thick layer of 3-m-diameter floes; and a mixture of 3-, 15-, 30-, and 60-m diameter floes. The river flow was simulated assuming a constant upstream discharge of 169 cms. Three downstream boundary conditions were used: normal flow at the downstream boundary; a downstream water surface elevation of 24.7 m relative to an arbitrary reference elevation that was independent of the flow rate; and a constant water surface elevation of 26.7 m, also independent of the flow rate. The results of simulations using the first two boundary conditions are not discussed here. The third boundary condition that is discussed simulates the condition of a major flood with the water level in the river at bankfull stage of 26.8 m. In each case the initial ice accumulation completely covered the surface of an 800 m stretch of river. The proposed bridge piers did not interrupt the passage of ice with the uniform-diameter small floes. Some thickening was observed at the piers, but there was no tendency to form an arch due to the large spacing between the piers relative to the floe diameter. However, with the ice cover composed of mixed floe diameters, blockage occurred when the largest 60-m-diameter floes were caught between widely spaced piers or between a pier and a bank. The passage of ice was completely stopped for bridge design 1 with 12 piers. The force levels developed by the small floes were relatively low and varied little with time. The force levels developed by the mixture of floes sizes were much higher and more variable. Force levels with the mixed floe sizes were higher because they impart a larger impulse during their initial collision with a pier and because when they are stopped by a pier they transmit the resultant of the forces exerted by all the floes pressing on their upstream perimeter as well as the water drag on their large bottom surface.

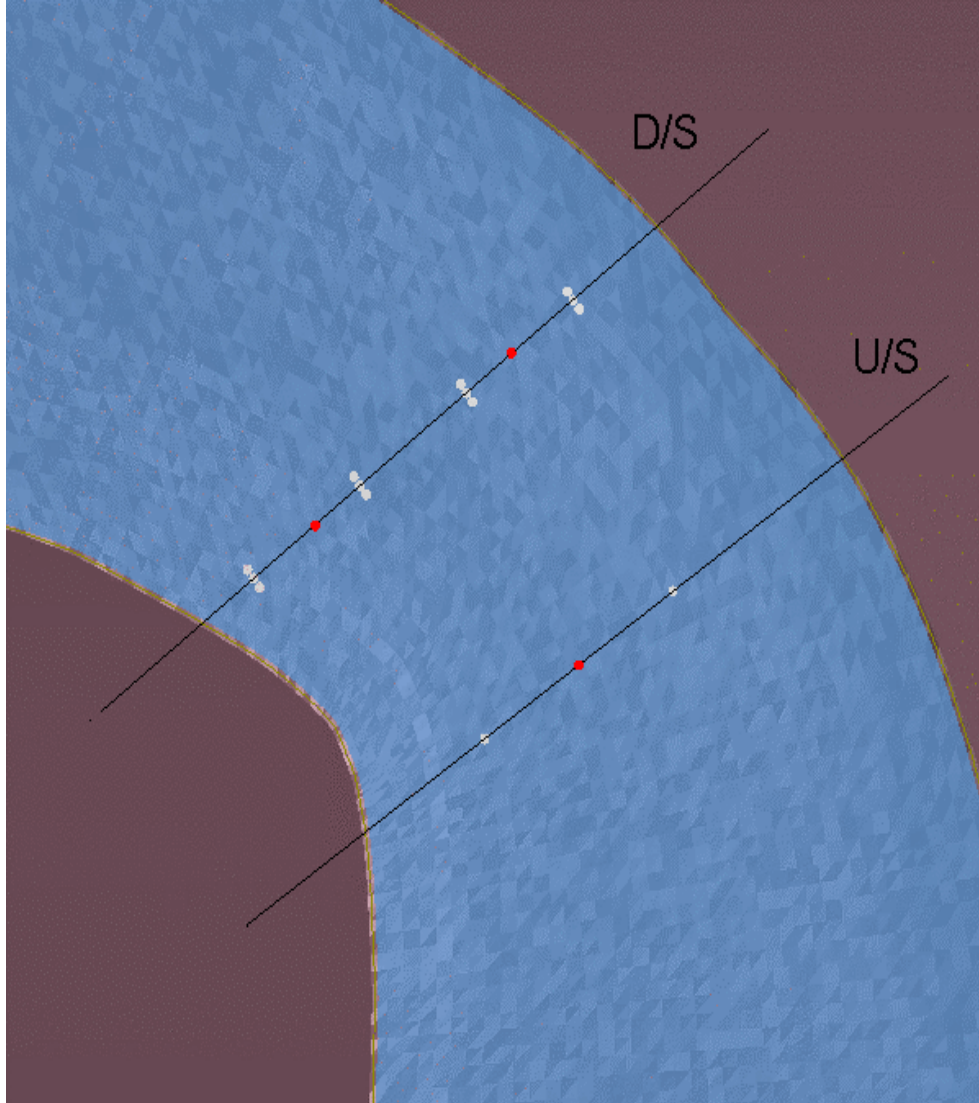


Figure 5. Bridge locations showing upstream and downstream section lines.

3. Describing Particle Motion

In this paper, a more complete description of the ice particle motion will be presented than in previous papers. The motion of a discrete ice floe can be described in a universal coordinate system by.

$$m_p \frac{dv_{pi}}{dt} = \mathbf{F}_i^f + \mathbf{F}_i^p + m_p \mathbf{g} \quad [1]$$

where v_{pi} = the floe velocity in the i th direction (here $i = x, y, z$ in the universal coordinate frame); m_p = the mass of the floe (the density is assumed uniform throughout); \mathbf{F}_i^f = the forces acting on

the floe in the i th direction due to the fluid; \mathbf{F}_i^p = the forces acting on the floe in the i th direction resulting from other floes; t = time; and \mathbf{g} = the gravity vector.

The ice floes in the simulations are flat disks with a circular edge. Dilating a flat disk of radius R_1 by a sphere with radius R_2 forms the floes. In the dilation process in mathematical morphology (Serra, 1986), the two-dimensional circular disk is transformed into a three-dimensional disk with thickness $h = 2R_2$ and diameter $d = 2(R_1+R_2)$ by placing a sphere with radius R_2 at every point on the two-dimensional circular disk. Changing R_1 and R_2 varies the aspect ratio of the floe d/h . The top and bottom surfaces of the floes are flat.

The force exerted on a floe by other floes in the i th direction can be found by summing the component of the normal forces, \mathbf{F}_n , and the tangential forces, \mathbf{F}_t , in the i th direction resulting from all contacts

$$\mathbf{F}_i^p = \sum^{All\ contacts} (\mathbf{F}_n n_i + \mathbf{F}_t t_i) \quad [2]$$

where n_i is the component of the normal to the plane of contact in the i th direction, and t_i is the component of the tangent to the plane of contact in the i th direction.

Wherever two floes touch, the overlap is interpreted as a deformation of the floes, resulting in a contact force. The contact force component normal to the surfaces at the point of contact \mathbf{F}_n is

$$\mathbf{F}_n = (k_n \delta - \eta \bar{V}_{1/2} \cdot \bar{\mathbf{n}}) \bar{\mathbf{n}} \quad [3]$$

The subscript n denotes the normal direction, k_n is the normal contact stiffness, η is the normal contact viscosity, and $V_{1/2}$ is the relative velocity of floe 1 with respect to floe 2 at the point of contact. A value of η near critical damping is used to produce highly inelastic behavior. Tensile forces are not modeled. The incremental change in the tangential force due to friction is proportional to the relative tangential velocity. The tangential force F_t at time m is calculated in terms of the force at the previous time step $m-1$ as

$$\mathbf{F}_t^m = \mathbf{F}_t^{m-1} - (k_t \Delta t (\bar{V}_{1/2} \cdot \bar{\mathbf{t}})) \bar{\mathbf{t}} \quad [4]$$

where Δt is the time step and k_t is the tangential contact stiffness that is set to 60% of k_n . If the tangential force \mathbf{F}_t exceeds the Coulomb limit $\mu|\mathbf{F}_n|$, where μ is the friction coefficient, the x , y , and z components of \mathbf{F}_t are scaled such that $|\mathbf{F}_t| = \mu|\mathbf{F}_n|$.

The forces acting on a floe in the i th direction due to the fluid are

$$\mathbf{F}_i^f = \frac{\rho_f}{\rho_s} \rho_f \frac{d\mathbf{V}_i}{dt} - m_{ii} \left(\frac{dv_{pi}}{dt} - \frac{d\mathbf{V}_i}{dt} \right) - \rho_f A_i C_{Di} (v_{pi} - \mathbf{V}_i) |v_{pi} - \mathbf{V}_i| - F_{i \text{ buoyancy}} \quad [5]$$

where the terms on the right side are the pressure force, the added fluid added mass, the fluid drag force, and the buoyancy force. Here \mathbf{V}_i = the fluid velocity in the i th direction, $\frac{\rho_f}{\rho_s}$ = the submerged volume of the particle; m = the added mass of the fluid; A_i = the effective cross-sectional area of the particle in the i th direction; C_{Di} = the drag coefficient in the i th direction;. The drag coefficient C_d , based on floe area, is 1.17 for flow normal to the flat surface and 0.1 for flow tangential to the flat surface (White, 1979). The buoyancy force is assumed to in the vertical direction. The components of buoyancy in the x and y direction arise only because of the slope of the water surface.

The rotation of the discrete element is calculated based on a frame of reference that is centered on and moves with the particle. This is accomplished by transforming from the universal to body frame using an adaptation of Evans singularity free quaternion approach (Evans and Murad 1977) as presented by Walton and Braun (1993). Euler's equation of rotation for a single floe is

$$I_i \frac{d\Omega_i}{dt} + \varepsilon_{ijk} \Omega_j \Omega_k I_k = \mathbf{M}_i^f + \mathbf{M}_i^p \quad [6]$$

where $\Omega^{\hat{i}}$ = the rotation rate around the \hat{i} th axis (here \hat{i} denotes a frame of reference centered and fixed to the ice floe); $I^{\hat{i}}$ = the moment of inertia about the \hat{i} th axis; \mathbf{M}_i^f = the moment acting on the particle about the \hat{i} th axis due to the fluid; \mathbf{M}_i^p = the moment acting on the particle about the i th axis due to other particles; and ε_{ijk} = the permutation symbol or Levi-Civita density (Goldstein 1980).

The moments due the interaction of floes is

$$\mathbf{M}_i^p = \sum^{All \text{ contacts}} (\mathbf{r}_i^p \times \mathbf{F}^T) \quad [7]$$

where $\mathbf{F}^T = \mathbf{F}_n + \mathbf{F}_t$; and \mathbf{r}_i^p = the moment arm from the \hat{i} th axis respectively and point of contact between two floes where \mathbf{F}^T acts.

The moments due to the fluid are determined as

$$\mathbf{M}_i^f = -I_{added \text{ mass } \hat{i}} \frac{d\Omega_i}{dt} - \iint_{ip \text{ axis}} (\mathbf{r}_i^D \times \mathbf{F}_{Di}) r dr d\phi + \mathbf{r}_i^B \times \mathbf{F}_{ibuoyancy} \quad [8]$$

where the terms of the right hand side are the moment of inertia of the added mass, the fluid drag resisting rotation; and the moment due to buoyancy. Here \mathbf{r}_i^B = the moment arm from the \hat{i} th axis respectively and the resultant vector of fluid pressure acting on the floe; and \mathbf{F}_D = the fluid drag force acting on the floe due to rotation over an area defined by $rdrd\phi$. We are assuming that the fluid velocity is always moving in straight lines parallel to the water surface; therefore the added mass and fluid drag moment calculations for a rotating floe need not account for the fluid velocity. The particles are symmetrical about all three-body axes; therefore the buoyancy cannot induce a moment unless the floe crosses the plane of the water surface in a non-symmetric manner.

4. Summary

In this paper we have reported on several recent advances in the use of DEM to simulate river ice. These advances include the use of multiple ice floes sizes, the development of an efficient spin-up procedure, and the complete description of the particle motion that includes all the relevant forces acting on the ice particles.

5. Reference:

- Daly, S.F., and M.A. Hopkins (2001) Estimating forces on an ice control structure using DEM. In Proceedings, 11th Workshop on the Hydraulics of Ice Covered Rivers, 14-16 May, 2001. Published on CD-ROM by the Committee on River Ice Processes and the Environment, Canadian Geophysical Union-Hydrology Section, Ottawa, Canada.
- Daly, S.F. and M.A. Hopkins (1999) Modeling River Ice using Discrete Particle Simulation. Proceedings of the 10th International Conference on Cold Regions Engineering, American Society of Civil Engineers, August 16-19, 1999, Lincoln, NH, pp. 612-622.
- Daly, S.F., and M.A. Hopkins (1998) Simulation of river ice jam formation. In Ice in Surface Waters, Proceedings of the 14th International Symposium on Ice, 27-31 July, Potsdam, New York (H.H. Shen, Ed.). Balkema.
- Evans, D.J. and S. Murad (1977) Singularity Free Algorithm for Molecular Dynamics Simulation of Rigid Polyatomics. *Mol. Phys.* **34**, p327.
- Goldstein, H. (1980) Classical Mechanics. Second Edition. Addison-Wesley Publishing Co. Reading, MA
- Hopkins, M.A., S.F. Daly, D.R. Shearer, and W. Townsend (2002) Simulation of river in a bridge design for Buckland, Alaska. Proceedings of the 16th International Symposium on Ice, Dunedin, New Zealand. 2-6 December 2002. Vol. I. pp. 254-261.
- Hopkins, M.A. and S.F. Daly (1999) Discrete Element Modeling of River Ice at Navigation Structures. Proceedings of the 10th Workshop on River Ice, The Canadian Committee on River Ice Processes and the Environment. June 8-11, 1999, Winnipeg, Manitoba, CA, pp 59-69.
- Hopkins, M.A., S.F. Daly, and J.H. Lever (1996) Three Dimensional Simulation of River Ice Jams. Proceedings of the American Society of Civil Engineers 8th International Conference on Cold Regions Engineering, August 13-16, 1996, Fairbanks, AK.

- Schlichting, H. (1979) *Boundary Layer Theory*. McGraw-Hill Book Company. New York, New York.
- Serra, J., Introduction to Mathematical Morphology (1986) *Computer Vision, Graphics, and Image Processing* 35, 283-305.
- Walton, O.R. and R.L. Braun (1993) Simulation of Rotary-Drum and Repose Tests for Frictional Spheres and Rigid Sphere Clusters. Joint DOE/NSF Workshop on FLOW OF PARTICULATES AND FLUIDS Sept. 29-Oct. 1, 1993, Ithaca, NY
- White, F.M., 1979, *Fluid Mechanics*, McGraw-Hill, New York.